Journal of Drug Design and Medicinal Chemistry
2024, Vol. 10, No. 3, pp. 67-80
https://doi.org/10.11648/j.jddmc.20241003.11

Research Article

In-Silico Screening of Prenylated Quercetin from *Globimetula oreophila* Against *Plasmodium falciparum* Enzymes: Hope for New Antimalarial Drugs

Dauda Garba[1, *], Jimoh Yusuf[2], Akande Amatul-Hafeez[2], Hassan Lukman Ali[2], Yakubu Muhammad Shamsudeen[2], Gidado Ibrahim[3], Rabiu Hafsat[2], Ismail Surayya Ibrahim[2], Tijani Omolara Tawakaltu[2], Olaiya Ayodele Akeem[2]

[1]Department of Pharmaceutical and Medicinal Chemistry, University of Abuja, Abuja, Nigeria
[2]Department of Pharmaceutical and Medicinal Chemistry, Ahmadu Bello University, Zaria, Nigeria
[3]Department of Chemistry, Federal College of Education, Yola, Nigeria

Abstract

Malaria continues to be one of the most devastating global health problems due to the high morbidity and mortality it causes in endemic regions. The search for new antimalarial targets is vital because of the increasing prevalence of drug resistance in malaria parasites. Malarial proteases constitute promising therapeutic targets as they play important roles in the parasite life cycle. The inhibition of these enzymes has pharmacological and therapeutic significance since they are involved in numerous processes, including the development, invasion, egress, and breakdown of host hemoglobin to release amino acids for parasite sustenance. In this study, *in silico* techniques were used to shed light on the mechanisms underlying the inhibitory effects of prenylated quercetin isolated from *Globimetula oreophila* on plasmepsin I and II, falciparum 2 and 3, *Plasmodium falciparum* calcium-dependent protein kinase 2, dihydrofolate reductase-thymidylate synthase, and serine repeat antigen 5. The test compound significantly interacts with key enzyme binding pockets through hydrogen bonds, van der Waals, and hydrophobic interactions, influencing protease specificity control. Crucial ligand features like carbonyl and hydroxyl groups were identified as essential for receptor interactions. Comparative analysis revealed the test compound's strong binding affinities with energies ranging from -6.4 Kcal/mol to -9.4 Kcal/mol, indicating competitive potential against various enzymes, particularly excelling against *Pf*DHFR-TS, plasmepsin-I, and SERA5 compared to native ligands. This suggests the compound's ability to competitively inhibit enzyme activity by targeting co-factor binding sites, especially with specific proteases, holding promise for therapeutic applications as potent inhibitors for the prevention and treatment of malaria.

Keywords

Globimetula oreophila, *In-silico*, Malaria, *Plasmodium falciparum*

[*]Corresponding author: dauda.garba@ymail.com (Dauda Garba)

Received: 8 August 2024; **Accepted:** 2 September 2024; **Published:** 30 September 2024

1. Introduction

Malaria is a common and life-threatening disease in many tropical and subtropical areas with staggering infection and mortality statistics [1]. A eukaryotic protist causes malaria; a single-celled organism and the parasite belongs to a genus known as *Plasmodium*. Species of the genus *Plasmodium* including *P. falciparum, P. vivax, P. ovale, P. malariae,* and *P. knowlesi* are known to cause malarial infection in humans [2]. *Plasmodium falciparum* can cause serious complications and can be fatal if untreated. It is responsible for the most deaths due to malaria [1]. In 2020, an estimated 241 million cases and 627,000 fatalities occurred worldwide, with sub-Saharan Africa accounting for the vast majority of cases and deaths—roughly 95% [1]. The resistance of malaria parasites to most of the widely used antimalarials is one of the main obstacles to controlling the disease. The only medications available today to treat chloroquine-resistant *Plasmodium falciparum* infections are artemisinins and artemisinin combination therapy (ACTs). Nonetheless, there have been reports of decreased ACT sensitivity in some Asian regions [1]. A primary hurdle in the development of novel antimalarial drugs lies in securing a promising lead compound with favorable pharmacokinetic attributes encompassing absorption, distribution, metabolism, excretion, and toxicity (ADMET).

Studies have shown that medicinal plants and their natural products have been identified as a robust source of medicinal properties due to secondary metabolites such as quinine and artemisinin, some of the most successful antimalarial agents. *Globimetula oreophila* commonly known as mistletoe belonging to the family of Loranthaceae, is found growing on dicotyledonous trees using them as a host for its root-like structure called haustoria [3]. Previous phytochemical screening of *G. oreophila* leaves crude extract and fractions were reported to be a rich source of secondary metabolites such as steroids/terpenoids, cardiac glycosides, saponins, tannins, flavonoids, and alkaloids [4, 5]. It was reported to be a rich source of essential trace metals in appropriate quantities [6].

Targeting a specific enzyme of the malaria parasite and modifying its metabolic pathway is a successful experimental technique for developing antimalarial drug candidates. Antimalarial drugs, both synthetic and natural, are designed to target the parasite's unique metabolic pathways in comparison to the host. The *Plasmodium* parasite feeds on 60–80% of the hemoglobin present in red blood cells during the intra-erythrocytic stage of its life cycle. It then dissolves the hemoglobin and uses the amino acids it contains for protein synthesis and energy. Hemoglobin breakdown may also be facilitated by giving the parasite the space it needs inside the erythrocyte to grow and reproduce. A cascade of aspartic proteases plasmepsins [7], cysteine proteases falcipains [8], and dihydrofolate reductase [9, 10] mediate massive degradation of host hemoglobin to release amino acids for parasite nutrition; (2) serine proteases (subtilases) have been implicated in erythrocyte invasion and parasite exit from the host [11, 12]; calcium-dependent protein kinase 2 important for calcium signaling at various stages of the parasite's life cycle they are attractive drug targets for malarial treatment and prevention.

In this study, we employed a computational approach that can be used to rationalize anti-malarial activities of compounds qualitatively and save time in evaluating the efficacy of these anti-malarial. [13]. The compounds were analyzed to help predict their absorption, distribution, metabolism, excretion, and toxicity (ADMET) properties. Based on the results of this study, it is expected that the compound may serve as a viable candidate for the development of proteases and kinase inhibitors that might be used to treat malaria. This study aims to evaluate the inhibitory activity of prenylated quercetin from *Globimetula oreophila* leaves extract on malaria-associated protein using an *in silico* docking study. The prospects of inhibition of *Plasmodium falciparum* vital enzyme; a cysteine protease (falcipain-2 and 3), aspartic protease (plasmepsin I and II), serine repeat antigen 5 (SERA5), *Plasmodium falciparum* dihydrofolate reductase thymidylate synthesis (PfDHFR-TS), and *Plasmodium falciparum* calcium-dependent protein kinase 2 (PfCDPK2) of 2-(3,4-dihydroxy-phenyl)-3-((5”-ethyl-2”-(2”’-hydroxypropyl)-3”-methynon-4”-en-1-yl)oxy)-5,7-dihydroxy-4”-H-chromen-4-one (DG1) isolated from the leave of *Globimetula oreophila* was investigated using *in silico* studies.

2. Material and Methods

2.1. Software, Hardware, and Databases

AutoDock Vina [14], MGL tools [14], UCSF Chimera [15], ChemDraw ultra.12, Discovery Studio, Spartan 04, SwissAdme (online server), Mac OSX, Windows (Intel processor, Corei5).

2.2. Protein Crystal Structures

High-resolution, non-mutant crystal structure files of the following enzymes from *P. falciparum* were obtained from RCSB Protein Data Bank (http://www.rcsb.org/pdb); Falcipain-2 [FP-2; PDB ID: 6SSZ] [16], Falcipain-3 [FP-3; PDB ID: 3BPM] [17], Plasmepsin-I [Plm-I; PDB ID: 3QS1] [18], Plasmepsin-II [Plm-II; PDB ID: 1LF3] [19], Serine Repeat Antigen-5 [SERA5; PDB ID: 6X42] [20], *Plasmodium falciparum* Calcium-Dependent Protein Kinase 2 [PfCDPK2; PDB ID: 4MVF] [21], and *Plasmodium falciparum* Dihydrofolate Reductase Thymidylate Synthase [PfDHFR-TS; PDB ID: 4DPD] [22].

2.3. *In-silico* Antimalarial Studies

2.3.1. Evaluation of Theoretical Oral Bioavailability

The oral bioavailability of the characterized compound DG1 was predicted theoretically based on Lipinski's rule of five, on the SWISSADME (http://www.swissadme.ch/index.php), and PROTOX-II https://tox.charite.de/protox3/ web serves were used for properties that defined the absorption, distribution, metabolism, excretion, and toxicity (ADMET) of the test compound respectively. Through extensive database utilization, the servers accurately predict a variety of physicochemical properties including lipophilicity, water solubility, pharmacokinetics, drug-likeness, medicinal attributes, and compound toxicity with remarkable precision.

2.3.2. Protein Structure Preparation

As mentioned, the crystal structures were obtained from the protein data bank (PDB). Before docking, residues located within 5.0Å around the native ligands. Chimera UCSF removed all crystallographic water molecules, ions, and bound ligands from the 3D structures retrieved from PDB [15]. The isolated receptors were prepared and saved as rec.pdb. AutoDock Tools [14] were used to edit the rec.pdb files by adding polar hydrogen and Gastegier charges and saving them as pdbqt files.

2.3.3. Ligand Structure Preparation

The 2D structure of the characterized compound (prenylated quercetin) was generated using ChemDraw ultra.12, and Spartan 04 was used to convert the 2D structures to 3D. Using the AMI semi-empirical method, geometrical optimization was carried out on all the compounds using the Spartan software, and the optimized structures were stored as mol2 files. AutoDock Tools was used to add hydrogen and Gastegier charges and saved as mol2 files to pdbqt format.

2.3.4. Molecular Docking Analysis

The docking procedure for each protease enzyme was validated before docking the test compounds by separating the co-crystallized ligand from the enzyme crystal structure and re-docking it using the set-up parameters. The procedure that gives conformation superimposable with a geometrical conformation of the co-crystallized ligand in the active site was chosen [23]. Before molecular docking, the active sites were defined according to the coordinates of the crystallographic structures of both enzymes by defining the grid box, and the best pose was obtained which was used for further studies. The UCSF Chimera was further used for post-docking visualization and pre-MD preparations of all systems (ligands and receptors).

3. Results and Discussion

3.1. Evaluation of Theoretical Oral Bioavailability

The theoretical oral bioavailability of the isolated compounds is presented in Table 1 with the molecular weight, hydrogen bond donor, hydrogen bond acceptor, number of rotatable bonds, and MLogP, values of the isolated compound for predicting theoretical oral bioavailability based on Lipinski's rule of five [24]. Topological Polar Surface Area (TPSA) and Molar Refractivity (MR) are other pharmacokinetic parameters studied.

Analyzing the drug's likeness makes finding and producing new drugs easier. The topological polar surface area (TPSA) and the molecular weight of the drug are important factors to take into account for it to pass across the biological barrier. The drug molecule can permeate less the higher the TPSA and molecular weight levels, and vice versa. Lipophilicity is defined as the partition coefficient logarithm of a drug/molecule in an organic or liquid phase (LogP). It improves the body's ability to break down medication candidates; hence, decreased digestion is seen by improved LogP. A drug compound's Log S value determines how well it dissolves; the lower the number, the better. The drug molecule's permeability, solubility, and bioavailability are suggested by Lipinski's five criteria [24].

Using a computational approach that reduces experiment time and cost, this Ro5 assists in the transition of an investigational novel drug from phase I to phase II [24, 25]. The rule of thumb of Lipinski states that orally administered drugs should possess a molecular weight under 500g/mol, 10 or fewer hydrogen bond acceptors, 5 or fewer hydrogen bond donors, and a log P less than 5. Any candidate's drug molecule that violates two or more of the rules would not be orally active. Based on the rule of Ro5, prenylated quercetin had a violation based on its molecular weight in Table 1 [24]. The drug's hydrophilicity is indicated by the logarithm of its partition coefficient between n-octanol and water, or log P-value. A lower log P indicates better drug molecule absorption within the cell. The drug molecule's solubility is shown by the Log S value, and a lower rate again replicates the candidate molecule's higher solubility. Topological polar surface area, or TPSA, is once more connected to the drug molecule's permeability and absorption. In a biological system, a medicinal molecule with a higher TSPA value frequently causes poor permeability. A targeted drug will be assessed by the synthetic accessibility (SA) score before being synthesized. The syntheses vary according to the distinct scores. For example, a score of 10 indicates extreme difficulty in synthesis, while a score of 1 indicates extreme ease of synthesis [26]. In addition to the bioavailability characteristics, the bioavailability score establishes a possible drug candidate's penetrability [27]. Prenylated quercetin (ligand) performed well in the drug-likeness prediction study and this

was evident when taking into account all phases of the study.

Table 1. *Analysis of theoretical oral bioavailability of compound DG1 based on Lipinski's rule of five Drug likeness prediction compound DG1.*

Properties	Prenylated quercetin
Formula	$C_{30}H_{38}O_8$
Mol.Wt[a]	526.62
#Heavy atoms	38
#Aromatic heavy atoms	16
Fraction Csp3	0.43
#HbA	8
#HbD	5
#nRB	12
MR	150.49
TPSA	140.59
MLogP	1.84
Lipinski violation[b]	Yes[1]
Inference	Pass
Ghose violations	4
Veber violations	2
Egan violations	2
Muegge violations	1
Bioavailability score	0.55
Synthetic accessibility	5.80

Molecular weight in g/mol, (b) Lipinski *et al.,* 2004 (Mwt≤500, MLogP≤4.15, N or O≤10, NH or OH≤5 and number of rotatable bonds≤ 10), nRB: Number of rotatable bonds, LogP: Partition coefficient, HbA: Hydrogen bond acceptor, HbD: Hydrogen bond donor, Topological Polar Surface Area (TPSA) ≤140 $Å^2$, MR: Molar Refractivity

3.2. ADMET Profile

As shown in Table 2, the water solubility values of prenylated quercetin represented in terms of log S_w were found to be -7.00 and predicted to be poorly water-soluble and the cytochrome P450 inhibitory potential of compound DG1. Lipophilicity was represented by the consensus log P values (arithmetic mean of iLOGP, XLOGP3, WLOGP, MLOGP, and Silicos-IT Log P values –Table 3) with a value of 5.08. Table 4 shows the toxicity profile compound DG1.

To assess a drug candidate's potential from both the pharmacological and pharmacodynamic perspectives within a biological system, we looked at ADMET predictions. As a result, the effectiveness of drug testing and enhancement is crucial, and for drugs that target brain cells, the blood-brain barrier (BBB) is essential. Furthermore, the intestinal mucosa must break down the drug molecules because a large portion of the drug is taken orally. P-glycoprotein (P-gp), a well-characterized ATP-binding cassette transporter in the plasma membrane, facilitates drug transfer and, as a result, inhibits P-gp and influences drug transportation. The Caco-2 cell line is utilized in permeability investigations conducted through in vitro analysis. The molecule's permeability determines whether or not the drug will be absorbed by the intestine. Based on the anticipated toxicity profile of the compound (DG1) in Table 3, prenylated quercetin is classified as an acute toxicity class V (LD_{50}≤5000 mg/kg) substance in Table 4 [28]. Prenylated quercetin does not tend to androgen, thyroid, estrogen receptor, and aromatase binding potential as shown in Table 2. Administered drugs go through the bloodstream and then return to the liver. After using the drugs as a substrate, an enzyme belonging to the cytochrome P450 family excretes the drug through the urine or bile. Drug degradation is the outcome of any form of interference with any of these enzymes [29]. When a molecule is shown to be a substrate for at least one kind of CYP450 enzyme, it means that the drug is anticipated to be broken down by the corresponding CYP450 enzyme or enzymes [30]. Human hepatotoxicity (H-HT) is a term used to describe a variety of liver damage that can result in the organ failing or even death [31]. To identify compounds that may be mutagenic, causing alterations or malignant growth, a mutagenicity test known as the Ames test is utilized. The Ames test system is a commonly used test to determine point mutations in deoxyribonucleic acid (DNA), such as modification, addition, or deletion of one or more base pairs [32]. In the digesting region, the ligand performed flawlessly. On the other hand, prenylated quercetin exhibits Caco-2 permeability while not being a p-gp inhibitor. The isolated compound DG1 was shown to be CYP2C19 and CYP3A4 inhibitors in the metabolism zone in Table 2, indicating a relatively easy ligand metabolism. The ligand examined in the Ames tests was not mutagenic or carcinogenic in the toxicity range and thus safe as shown in Table 4.

Table 2. *Pharmacokinetics Prediction output and oral bioavailability of compound DG1.*

Properties	Prenylated quercetin
Silicos-IT LogSw	-7.00
Silicos-class	Poorly soluble
Consensus Log P	5.08
Log Kp (cm/s)	-4.48
GI Absorption	Low

Properties	Prenylated quercetin
BBB Permeant	No
Pgp substrate	No
CYP1A2 inhibitor	No
CYP2C19 inhibitor	Yes
CYP2C9 inhibitor	No
CYP2D6 inhibitor	No
CYP3A4 inhibitor	yes

Properties	Prenylated quercetin
Ames mutagenesis	-
Carcinogenicity	-
Hepatotoxicity	-
Androgen receptor binding	-
Thyroid receptor binding	-
Estrogen receptor binding	-
Aromatase binding	-

-: inactive; +: active; Class IV: LD_{50}≤2000 mg/kg; Class V: LD_{50}≤5000 mg/kg; Class VI: LD_{50}>5000 mg/kg

Table 3. Consensus log P values of compound DG1.

Properties	Prenylated quercetin
iLOGP	3.98
XLOGP3	7.09
WLOGP	6.21
MLOGP	1.84
Silicos-IT Log P	6.26
Consensus Log P	5.08

Table 4. Toxicity profile of compound DG1.

Properties	Prenylated quercetin
Oral Acute Toxicity	Class V

3.3. Molecular Docking Studies

3.3.1. Grid Box

The configuration file (config.txt) was tailored according to the grid box parameter, resulting in AutoDock Vina generating outputs in pdbqt format. Employing Chimera's ViewDock feature, we pinpointed compounds exhibiting superior binding energy, ideal geometric conformations, and wide-ranging inhibitory effects across all studied enzymes. These compounds were stored in complexes alongside the reference enzymes. The preparation of enzymes and DG1 (ligand) for each system was meticulously carried out using Chimera, following the methodology outlined by Pettersen and colleagues [15]. Details of the grid box parameter can be found in Table 5.

Table 5. Grid box parameter for the enzymes.

Enzyme	Grid Box Size			Center		
	X	Y	Z	X	Y	Z
Falcipain-2	40	40	40	19.2868	-40.6414	8.8792
Falcipain-3	16	16	24	5.95	-22.364	50.067
Plasmepsin I	44	40	40	27.55	-9.925	4.252
Plasmepsin II	40	40	40	16.215	6.85	27.605
PfDHFR-TS	40	40	48	24.614	4.953	58.236
Serine Repeat Antigen-5	10	10	10	-39.347	2.082	-34.907
Calcium Dependent Protein Kinase-1	40	40	40	32.333	85.018	21.838

3.3.2. Validation of Docking Procedures

The docking procedures applied to the seven enzymes were well-validated, as shown in Table 6. All the co-crystallized ligands re-docked on their respective proteins, and are well superimposed on their original Protein Data Bank (PDB) structures.

Table 6. *The crystal structures of enzyme complexes and re-docked ligands super-imposed on the crystal structures for validation.*

Enzyme Code and name	Crystal structure complex (Enzyme and Native Ligand)	Crystal structure complex (Enzyme, Native Ligand and Re-docked ligand) (Validation)
Falcipains-2 (6SSZ)	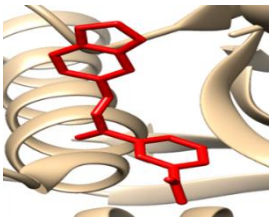	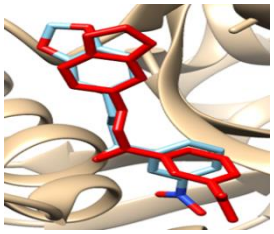
Falcipains-3 (3BPM)	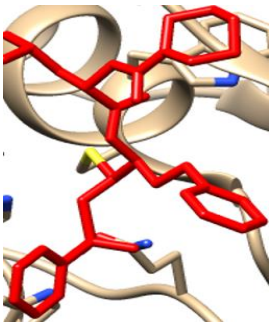	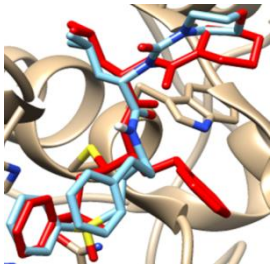
Plasmepsin I (3QSI)	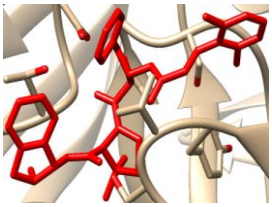	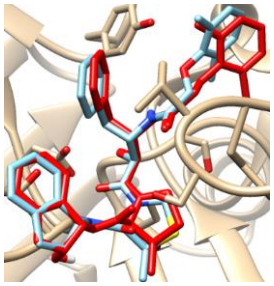
Plasmepsin II (1LF3)	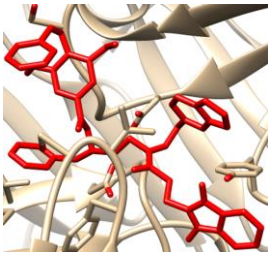	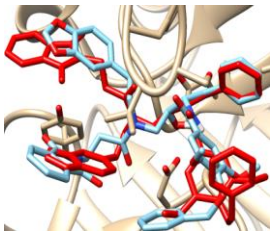
Serine Repeat Antigen 5 (6X42)	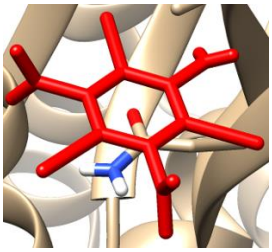	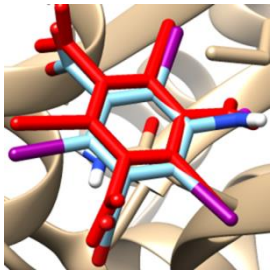
Calcium Dependent Protein Kinase-2 (MVF)	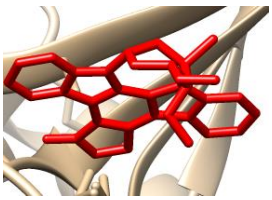	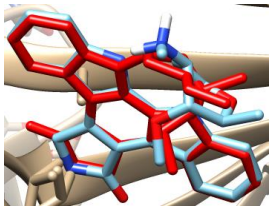

Enzyme Code and name	Crystal structure complex (Enzyme and Native Ligand)	Crystal structure complex (Enzyme, Native Ligand and Re-docked ligand) (Validation)
Plasmodium falciparum Dihydrofolate Reductase	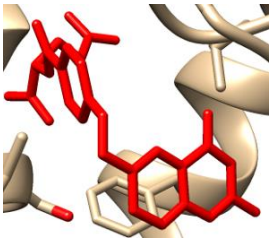	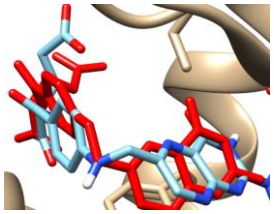

3.3.3. Binding Affinity of Ligand to the Protease Enzymes

The binding energies of the co-crystallized ligands and the prenylated quercetin against protease enzymes are presented in Table 7.

The result obtained from the molecular docking analysis demonstrated that the test compound was found to interact with the residues at the active site and other sub-unites regulating the specificity of the proteases. The test compound has a better binding affinity within the binding pockets of falcipain-2, falcipain-3, Plasmepsin I, Plasmepsin II, *Pf*CDPK2, *Pf*DHFR, and SERA5 and it is which is evident that the binding process where principally favored by hydrogen bond, van der Waals and other hydrophobic interactions. With regards to the binding interactions, the most contributing features of the ligands for receptor interactions are the carbonyl group, hydroxyl group, methyl group, and oxymethylene group. Table 7 shows the binding affinities of the test compound and the standard ligands. Based on the docking score of the various enzymes under study, the dihydrofolate reductase had the lowest energy and thus, the highest binding affinity as compared to other proteases with prenylated quercetin. From Table 7, it was seen that the order of increasing binding energy with the various ligands is *Pf*DHFR-TS (-9.4 Kcal/mol)>Plm-I (-8.2 Kcal/mol)>*Pf*CDPK2 (-7.9 Kcal/mol)>Plm-II (-7.2 Kcal/mol)>Fla-3 (-6.7 Kcal/mol)>Fal-2 (-6.5 Kcal/mol)>SERA5 (-6.4 Kcal/mol). The binding energy of the test compound with the various enzymes ranges from -6.4 Kcal/mol to -9.4 Kcal/mol while it was -3.4 to -11.3 for the native ligands. Additionally, the native ligands in all the *plasmodium falciparum* enzymes had a higher binding affinity than that of the test compound except in *Pf*DHFR-TS, Plm-I, and SERA5 where the test compound had a higher binding affinity. This suggests the potential ability of the compound to compete with various proteases under study for the co-factor binding site of the enzyme leading to inhibition of its activity.

Table 7. *The binding energies of the co-crystallized ligands and compound DG1 against malaria protease enzymes.*

Enzyme	Lig0 Affinity (Kcal/mol)	Lig1 Affinity (Kcal/mol)
Falcipain-2	-7.4	-6.5
Falcipain-3	-6.9	-6.7
Plasmepsin I	-10.2	-8.2
Plasmepsin II	-10.0	-7.2
*Pf*DHFR-TS	-9.4	-9.4
Serine Repeat Antigen-5	-3.4	-6.4
Calcium Dependent Protein Kinase-2	-11.3	-7.9

Lig0 (falcipin-2): - (~{E})-3-(1,3-benzodioxol-5-yl)-1-(3-nitrophenyl) prop-2-en-1-one (JV1); falcipain-3: N~2~-(morpholin-4-ylcarbonyl)-N-[(3S)-1-phenyl-5-(phenylsulfonyl) pentan-3-yl]-L-leucinamide (C1P); Plasmepsin-I: (4R)-3-[(2S,3S)-3-{[(2,6-dimethylphenoxy)acetyl]amino}-2-hydroxy 4 phenylbutanoyl] N [(1S,2R)-2-hydroxy-2,3-dihydro-1H-inden-1-yl]-5,5-dimethyl-1,3-thiazolidine-4-carboxamide(006); plasmepsin-II: N-(1-benzyl-3-{[3-(1,3-dioxo-1,3-dihydro-isoindol-2-yl)-propionyl]-[2-(hexahydro-benzo[1,3]dioxol-5-yl)-ethyl]-amino}-2-hydroxy-propyl)-4-benzyloxy-3,5-dimethoxy-benzamide (EH58); PfDHFR: Dihydrofolic acid (DHF); amino-2,4,6-triiodobenzene-1,3-dicarboxylic acid (I3C); amino-2,4,6-triiodobenzene-1,3-dicarboxylic acid (I3C); Lig1: DG1 (Prenylated quercetin).

3.3.4. The Binding Poses and Binding Interactions Analysis of Prenylated Quercetin Against Plasmodium Falciparum Enzymes

The binding conformation and interaction of prenylated quercetin with residues on the active site of the falcipain-2 falcipain-3, plasmepsin I, plasmepsin II, CDPK2, SERA5, and *Pf*DHF-TS studied using Chimera [15] and Discovery Studio Suite (www.accelrys.com) are shown on Figures 1-7.

Figures 1-7 shows the three-dimensional (3D) and two-

dimensional (2D) representations of the binding conformation and interactions analysis of the test compound with active sites of falcipain 2 and 3, plasmepsin I and II, *Plasmodium falciparum* dihydrofolate reductase thymidylate synthase (*Pf*DHFR-TS), *Plasmodium falciparum* calcium-dependent protein kinase 2 (*Pf*CDPK2), and serine repeat antigen 5 (SERA5) studied using Chimera [15] and Discovery Studio Suite (www.accerlrys.com). The test compound was seen to occupy the native ligand binding site of the enzyme. From the molecular interactions of falcipain 2 with Compound DG1, 3 hydrogen bonds were formed through the ortho-substituted hydroxyl group of the phenyl ring, carbonyl carbon of the central ring, and the oxymethylene of the prenylated side chain with the enzyme target, including Cys22, Asn21, and Asp18 (Figure 1; Table 8). Additionally, compound DG1 was stabilized through hydrophobic interactions with amino acid residues such as Val135, Asp137, Ser136, Ala140, Lys20, Trp189, Trp193, Gln19, Asn156, Gly23, His157, and Cys22 (2-bonds). Compound DG1 formed 4 hydrogen bonds through two ortho-substituted hydroxyl groups of the phenyl ring, carbonyl carbon of the central ring, and the hydroxyl group of the prenylated side chain with the falcipain 3 at the active site, including Cys51 Glu243 Gly42 Gly92 (Figure 2; Table 8). Hydrophobic interactions were predicted between Falcipain 3 and compound DG1 with residues Ala184 Asn182 Trp52 Ile94 Cys51[a] His183 Gln45 Trp215 Ala166 Ala161 yr90 Cys89 Gly91 Pro181 Tyr93 which involves in stabilization of ligand through protonation and deprotonation event within the active site of falcipain 3. Compound DG1 formed 4 hydrogen bonds through one ortho-substituted hydroxyl group of the phenyl ring, one hydroxyl group of the prenylated side chain, and the carbonyl carbon of the central ring with plasmepsin I enzyme, including Ser219 (2-bonds), Thr218, and Gly34 (Figure 3; Table 8). Additionally, compound DG1 was stabilized through hydrophobic interactions with amino acid residues Ile213 Val12 Met13 Ile30 Phe117 Ala111 Gly217 Ser77 Asp32 Tyr75 Ser35 Ser220 Ile287 Asp215 Thr222 Ile300 Val289 Val76 Leu291 Tyr189 (Figure 3; Table 8). Compound DG1 formed 2 hydrogen bonds through one ortho-substituted hydroxyl group of the aromatic ring and one hydroxyl group of the prenylated side chain with the plasmepsin II enzymes, including Ser218 and Asp34 (Figure 4; Table 8). The amnio acid residue Asp34 is one of the catalytic dyads of the plasmepsin II and was seen to form a hydrogen bond with the hydroxyl group of the aromatic ring which is responsible for the inhibition of the parasite thereby displacing the water molecule from the active site and Ser218 group occupies the pockets. This has an impact on the disruption of the life cycle of the *Plasmodium Falciparum* parasite. Hydrophobic interactions predicted between Plm II and compound DG1 with residue Leu292 Ile290 Thr221 Val78[b] Tyr192 Gly36 Ser37 Asp214 Thr114 Ser79 Thr217 Gly216 Tyr77 Phe120 Phe111 Ile123 Ala219 Ile32 which can enhance the selectivity of the compound by optimizing its fit and complementarity to the target (Figure 4; Table 8). Compound DG1 formed 3 hydrogen bonds through two ortho-substituted hydroxy groups in one aromatic ring and one hydroxyl group with the side chain with *Plasmodium falciparum* calcium-dependent protein kinase 2 (*Pf*CDPK2), including Glu153 (2-bonds) and Gln80 (Figure 5; Table 8). Hydrophobic interactions predicted between Plm II and compound DG1 with residues Glu196, Gly79, Val130, Ala99, Cys149, Glu147, Ile212, Leu148, Leu199, Val86, Lys101, Gly81, Thr82, Asp213, Asn197, Asp192, and Lys194 (Figure 5; Table 8) which enhance the selectivity of the compound by optimizing its fits and complementary to the target. Compound DG1 formed 4 hydrogen bonds through one ortho-substituted hydroxyl group in each of the aromatic rings and one carbonyl carbon group of the central ring with *Plasmodium falciparum* dihydrofolate reductase thymidylate synthase (*Pf*DHFR-TS) enzymes, including Asp54, Ser11 (2-bonds), and Ser108. Additionally, compound DG1 was stabilized by hydrophobic interactions with amino acid residues Arg122, Cys59, Pro113, Ile112, Leu119, Met55, Val45, Phe58, Tyr57, Ile14, Ala16, Cys15, Leu46 (2-bonds), Tyr170, Leu40, Ser167, Val195, Gly165, Gly41, and Phe116 (Figure 6; Table 8). Compound DG also formed 3 hydrogen bonds through two ortho-substituted hydroxyl groups in one aromatic ring and a carbonyl carbon of the central ring with serine repeat antigen 5 (SERA5), including Tyr772, Lys780, and Ser781 (Figure 7; Table 4). Hydrophobic interactions predicted between Plm II and compound DG1 with residues Asn771 Lys779 Glu570 Lys723 Val719 Asp716 Tyr804 Lys780 (Figure 7; Table 8) which involve in stabilization of ligands through protonation and deprotonation event within the active site of the enzyme.

The formation of multiple bonds observed between compound DG1 with all the enzymes under study increases the complexes' stability and contributes to higher binding affinity. From this study, it has been shown that the compound has interactions with active amino acid residues within the different receptors studied, our findings, therefore, imply that the compound may have the potential to modify the active site of the enzymes so the *plasmodium falciparum* enzymes binding is prevented. Therefore, this could interfere with the function of the malaria-associated enzymes and then cause inhibition of their activity. The common structural features of the compound were the presence of ortho hydroxyl, carbonyl carbon, and prenylated side chain with the nucleus of the molecule which is thought to impart the ability to inhibit the *Plasmodium falciparum* enzymes under study. The presence of hydrogen bonds in the docked protein-ligand complex as shown in Figures 1-7, is of interest because hydrogen bonds are usually seen to be facilitators of protein-ligand binding such as functional group interactions which can form specific interactions with complementary residues in the target receptor, enhancing the selectivity of the drug molecules. The carbonyl carbon which is involved in hydrogen bonding in the active site, is thought to contribute to solubility. Addi-

tionally, other types of interactions (van der Waals, and electrostatic charge) are a good indication of good docking quality and complex stability which was observed in this study. The bulky side chain in compound DG1 is more favorable than the smaller side chain group in ligand-protein interactions as suggested by structure-activity relationships (SARS) [32, 33].

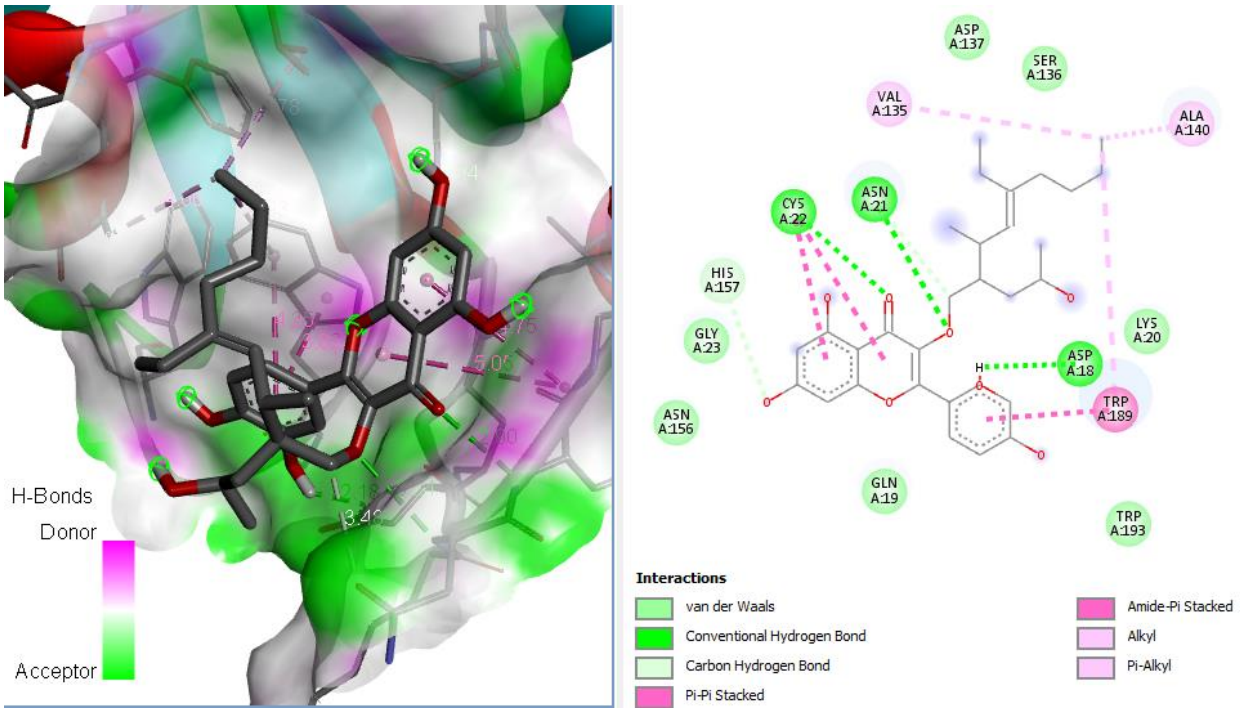

Figure 1. *3D molecular pose and 2D interactions of DG1 on the binding cavity of Falcipain 2 showing 2D (left) and 3D (right) views.*

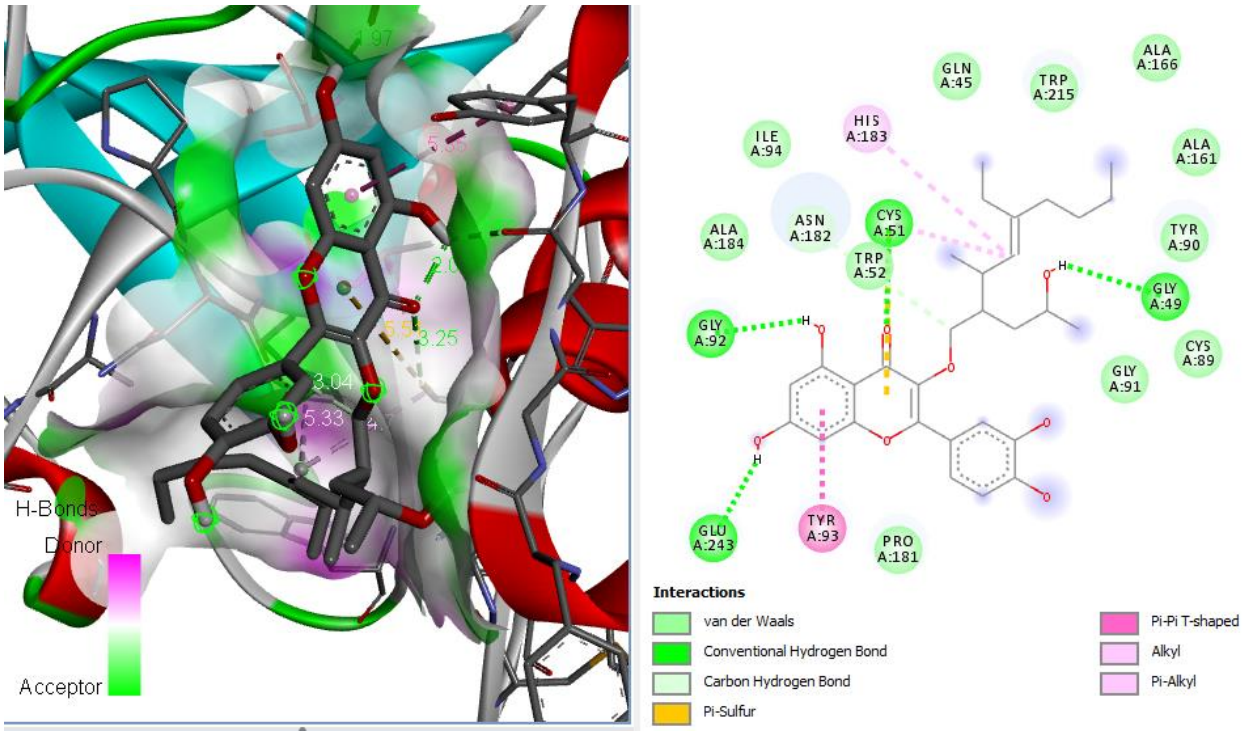

Figure 2. *3D molecular pose and 2D interactions of DG1 on the binding cavity of Falcipain 3 showing 2D (left) and 3D (right) views.*

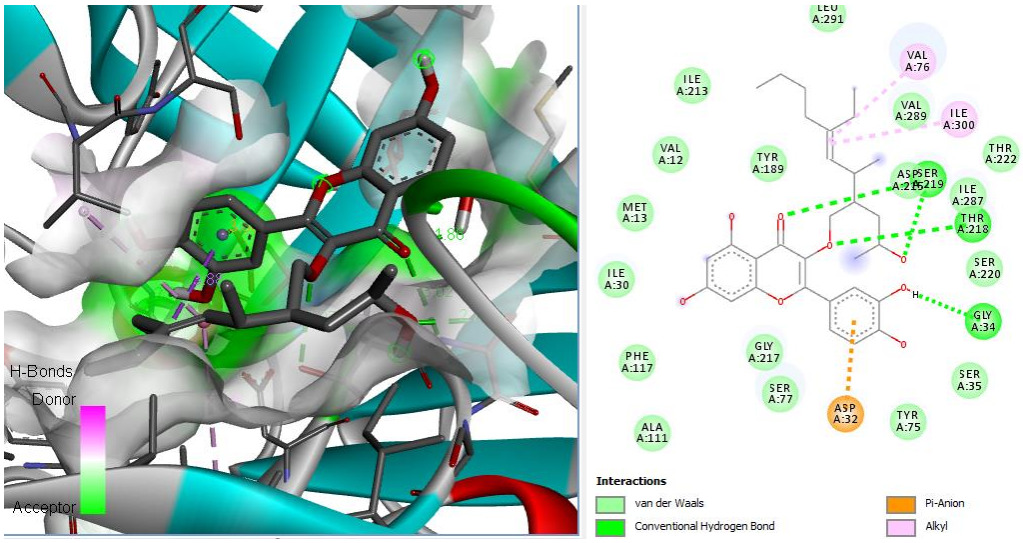

Figure 3. *3D molecular pose and 2D interactions of DG1 on the binding cavity of Plasmepsin I showing 2D (left) and 3D (right) views.*

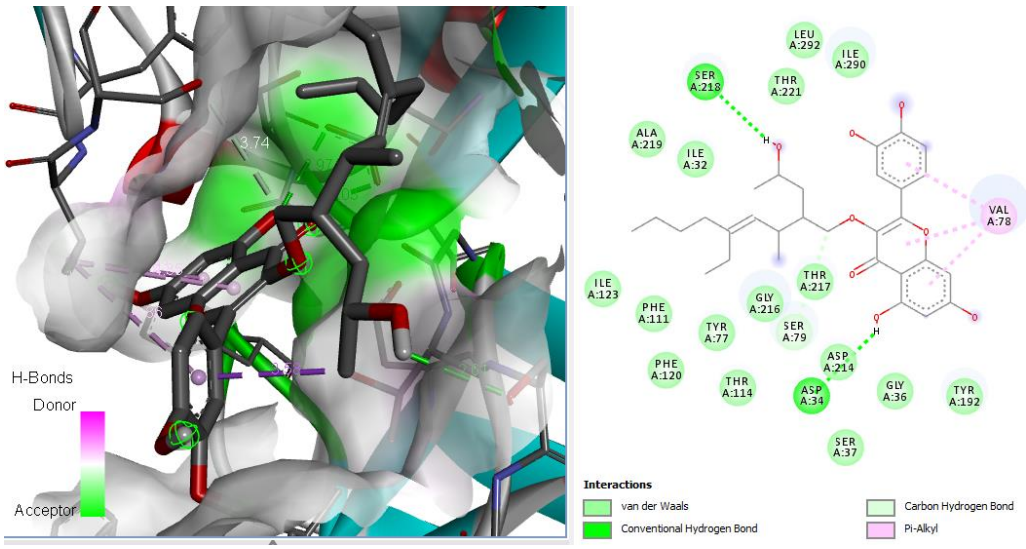

Figure 4. *3D molecular pose and 2D interactions of DG1 on the binding cavity of Plasmepsin II showing 2D (left) and 3D (right) views.*

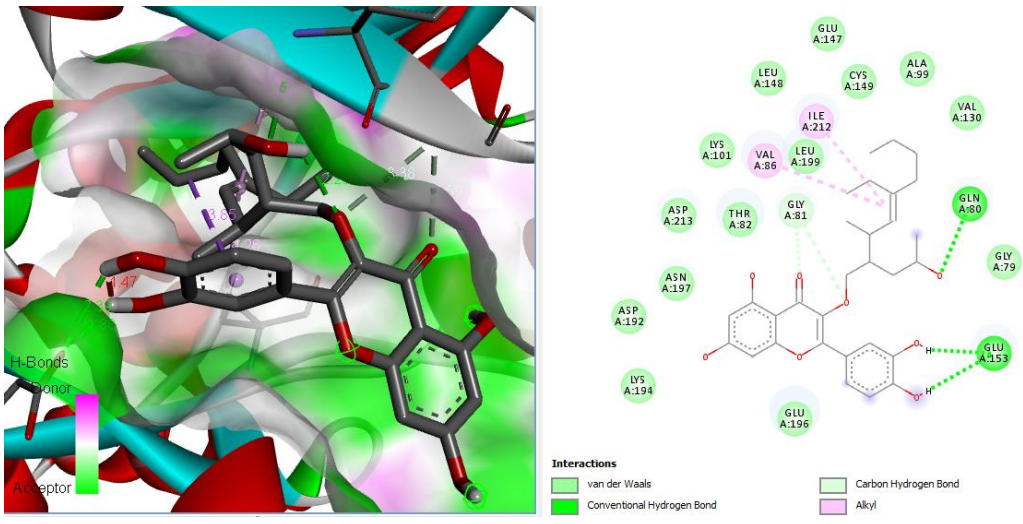

Figure 5. *3D molecular pose and 2D interactions of DG1 on the binding cavity of Calcium Dependent Protein Kinase-2 showing 2D (left) and 3D (right) views.*

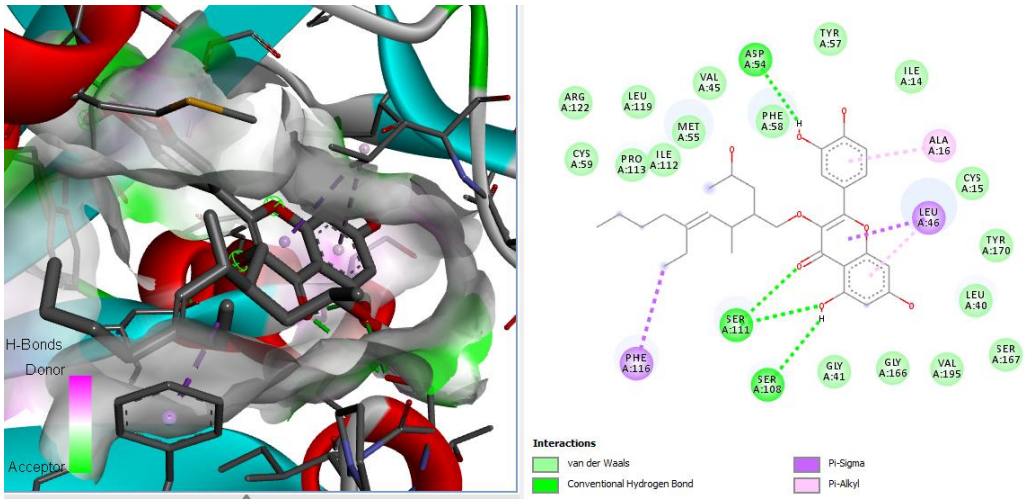

Figure 6. 3D molecular pose and 2D interactions of DG1 on the binding cavity of Plasmodium falciparum Dihydrofolate Reductase Thymidylate Synthase showing 2D (left) and 3D (right) views.

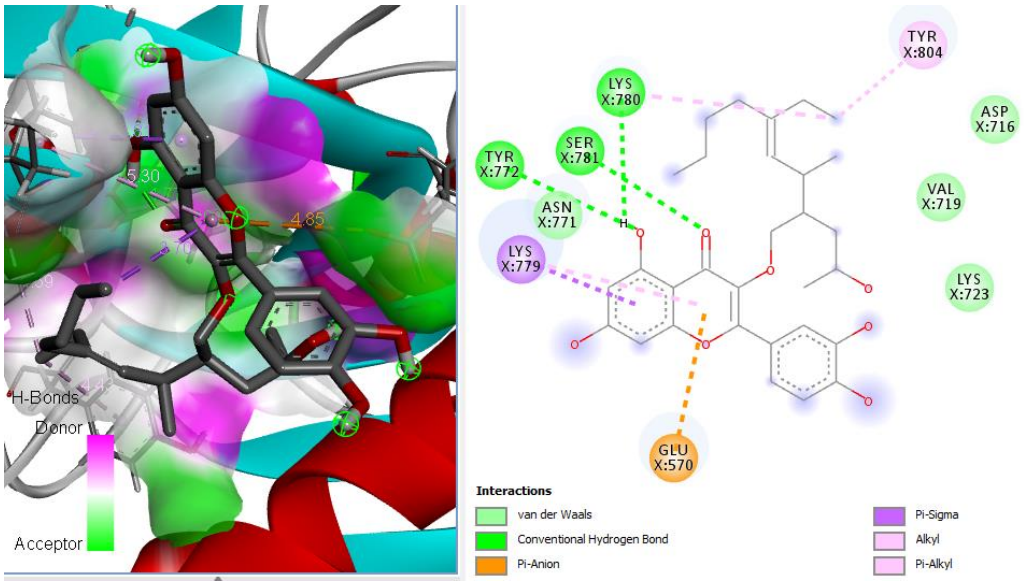

Figure 7. 3D molecular pose and 2D interactions of DG1 on the binding cavity of Serine Repeat Antigen-5 showing 2D (left) and 3D (right) views.

Table 8. Molecular interactions of the amino acid residues of compound DG1 with crystal structures of Plasmodium falciparum vital enzyme; a cysteine protease (falcipain-2 and 3), aspartic protease (Plm-I and II), PfCDPK2, PfDHFR, and SERA5.

Protein	Compound	Hydrogen Bond Interaction		Hydrophobic Interaction	
		Numbers	Amino acid	Numbers	Amino acid Residues
Falcipain-2 (6SSZ)	DG1	3	Cys22 Asn21 Asp18	13	Val135 Asp137 Ser136 Ala140 Lys20 Trp189 Trp193 Gln19 Asn156 Gly23 His157 Cys22[a]
Falcipain-3 (3BWK)		4	Cys51 Gly49 Glu243 Gly92	16	Ala184 Asn182 Trp52 Ile94 Cys51[a] His183 Gln45 Trp215 Ala166 Ala161 yr90 Cys89 Gly91 Pro181 Tyr93
Plasmepsin I (3QS1)		4	Ser219[a] Thr218 Gly34	20	Ile213 Val12 Met13 Ile30 Phe117 Ala111 Gly217 Ser77 Asp32 Tyr75 Ser35 Ser220 Ile287 Asp215 Thr222 Ile300 Val289 Val76 Leu291 Tyr189

Protein	Compound	Hydrogen Bond Interaction		Hydrophobic Interaction	
		Numbers	Amino acid	Numbers	Amino acid Residues
Plasmepsin II (1LF3)		2	Ser218 Asp34	20	Leu292 Ile290 Thr221 Val78[b] Tyr192 Gly36 Ser37 Asp214 Thr114 Ser79 Thr217 Gly216 Tyr77 Phe120 Phe111 Ile123 Ala219 Ile32
*Pf*CDPK2 (4MVF)		3	Glu153[a] Gln80	17	Glu196 Gly79 Val130 Ala99 Cys149 Glu147 Ile212 Leu148 Leu199 Val86 Lys101 Gly81 Thr82 Asp213 Asn197 Asp192 Lys194
*Pf*DHFR-TS (4DPD)		4	Asp54 Ser111[a] Ser108	21	Arg122 Cys59 Pro113 Ile112 Leu119 Met55 Val45 Phe58 Tyr57 Ile14 Ala16 Cys15 Leu46[a] Tyr170 Leu40 Ser167 Val195 Gly165 Gly41 Phe116
SERA5 (6X42)		3	Tyr772 Ser781 Lys780	8	Asn771 Lys779 Glu570 Lys723 Val719 Asp716 Tyr804 Lys780

a: two bonds; b: three bonds

4. Conclusion

This research delved into investigating the therapeutic promise of prenylated quercetin as a potential candidate for addressing malaria-associated enzymes via molecular docking analysis. The results highlight how this natural compound can engage with distinct malaria targets, indicating their potential as antimalarial agents. The inhibition of these enzymes by the isolated compound could offer therapeutic benefits against *Plasmodium falciparum* and as a good candidate for new sources in the development of antimalarial drugs.

Abbreviations

ADMET	Absorption, Distribution, Metabolism, Excretion, and Toxicity
DNA	Deoxyribonucleic Acid
SA	Synthetic Accessibility
G.	*Globimetula*
*Pf*CDPK2	*Plasmodium falciparum* Calcium-Dependent Protein Kinase 2
*Pf*DHFR-TS	*Plasmodium falciparum* dihydrofolate reductase thymidylate synthase
PDB	Protein Data Bank
TPSA	Topological Polar Surface Area
MR	Molar Refractivity
SERA5	Serine Repeat Antigen 5

Author Contributions

Dauda Garba: Conceptualization, Formal Analysis, Investigation, Methodology, Project administration, Resources, Supervision, Validation, Writing – original draft, Writing – review & editing

Jimoh Yusuf: Conceptualization, Formal Analysis, Methodology, Software, Writing – original draft, Writing – review & editing

Akande Amatul-Hafeez: Formal Analysis, Methodology, Validation, Visualization

Hassan Lukman Ali: Investigation, Project administration, Resources, Software, Validation

Yakubu Muhammad Shamsudeen: Conceptualization, Methodology, Validation, Writing – original draft, Writing – review & editing

Gidado Ibrahim: Investigation, Project administration, Resources, Software, Supervision, Validation

Rabiu Hafsat: Project administration, Software, Supervision, Writing – original draft

Ismail Surayya Ibrahim: Formal Analysis, Methodology, Project administration, Validation, Visualization

Tijani Omolara Tawakaltu: Formal Analysis, Project administration, Resources, Software, Visualization

Olaiya Ayodele Akeem: Methodology, Supervision, Visualization, Writing – original draft, Writing – review & editing

Conflicts of Interest

The authors declare no conflicts of interest.

References

[1] World Health Organization. World Malaria Report (2022); World Health Organization: Geneva, Switzerland, 2022.

[2] Smyth JD (1994) Animal Parasitology. Cambridge University Press, New York, p. 549.

[3] Burkill HM (1985) The useful plants of West Tropical Africa vol. 4 Royal Botanical Gardens, Kew, Richmond UK. ISBN 9780947643010.

[4] Dauda G, Haruna AK, Musa AM, Hassan B, Mohammed IM, Magaji MG (2016) *In-vivo* antimalarial activity of ethanol leaf extract of *Globimetula oreophila* (Hook. F) Danser *Azadirachta Indica.* BioL Environ Sci J Trop 13: 55-59.

[5] Dauda G, Ali BH, Muhammed SY, Muhammad MG, Ismail AM, Muhammad MA, Hassan HS (2023) Qualitative and quantitative phytochemical profiling of ethnomedicinal folklore plant-*Globimetula oreophila*. J Curr Biomed Res 3: 1407-26.

[6] Dauda G, Ali BH, Muhammad SY, Muhammed MG, Muhammad MA, Hassan HS (2023b) Levels of trace metals content of crude ethanol leaf extract of G*lobimetula oreophila* (Hook. f) Danser growing on *Azadirachta indica* using atomic absorption spectroscopy. J Curr Biomed Res 3: 1397-1406.

[7] Coombs GH, Goldberg DE, Klemba M, Berry C, Kay J, Mottram JC (2001) Aspartic proteases of *Plasmodium falciparum* and other parasitic protozoa as drug targets. Trends Parasitol 17: 532-537.

[8] Rosenthal PJ (2004) Cysteine proteases of malaria parasites. Int J Parasitol 34: 1489-1499.

[9] Murata CE, Goldberg DE (2003) *Plasmodium falciparum* falcilysin: a metalloprotease with dual specificity. J BioL Chem 278: 38022-38028.

[10] Eggleson KK, Duffin KL, Goldberg DE (1999) Identification and characterization of falcilysin, a metallopeptidase involved in hemoglobin catabolism within the malaria parasite *Plasmodium falciparum*. J Biol Chem 274: 32411-32417.

[11] Withers-Martinez C, Jean L, Blackman MJ (2004) Subtilisin-like proteases of the malaria parasite. Mol Microbiol 53: 55-63.

[12] Blackman MJ (2008) Malarial proteases and host cell egress: an 'emerging' cascade. Cell Microbiol 10: 1925-1934.

[13] Makrynitsa GI, Lykouras M, Spyroulias GA, Matsoukas MT (2018) *In silico* Drug Design. In: eLS. John Wiley and Sons, Ltd: Chichester. pp 1-7.

[14] Morris GM, Huey R, Lindstrom W, Sanner MF, Belew RK, Goodsell DS, Olson AJ (2009) AutoDock4 and AutoDockTools4: Automated docking with selective receptor flexibility. J Comput Chem 30: 2785–2791.

[15] Pettersen EF, Goddard TD, Huang CC, Couch GS, Greenblatt DM, Meng EC, Ferrin TE (2004) UCSF Chimera—a visualization system for exploratory research and analysis. J Comput Chem 25: 1605-1612.

[16] Machin JM, Kantsadi AL, Vakonakis I (2019) The complex of *Plasmodium falciparum* falcipain-2 protease with an (E)-chalcone-based inhibitor highlights a novel, small, molecule-binding site. Malar J 18: 1-9.

[17] Kerr ID, Lee JH, Pandey KC, Harrison A, Sajid M, Rosenthal PJ, Brinen LS (2009) Structures of falcipain-2 and falcipain-3 bound to small molecule inhibitors: implications for substrate specificity. J Med Chem 52: 852-857.

[18] Bhaumik P, Horimoto Y, Xiao H, Miura T, Hidaka K, Kiso Y, Wlodawer A, Yada RY, Gustchina A (2011) Crystal structures of the free and inhibited forms of plasmepsin I (PMI) from Plasmodium falciparum. J Struct BioL 175: 73-84.

[19] Asojo OA, Gulnik SV, Afonina E, Yu B, Ellman JA, Haque TS, Silva AM (2003) Novel uncomplexed and complexed structures of plasmepsin II, an aspartic protease from *Plasmodium falciparum*. J Mol Biol 327: 173-181.

[20] Smith NA, Clarke OB, Lee M, Hodder AN, Smith BJ (2020) Structure of the *Plasmodium falciparum* PfSERA5 pseudozymogen. Prot Sci 29: 2245-2258.

[21] Lauciello L, Pernot L, Bottegoni G, Bisson W, Scapozza L, Perozzo R (To be published) *P. falciparum* Calcium-Dependent Protein Kinase 2 (PfCDPK2): First Crystal Structure and Virtual Ligand Screening. https://www.rcsb.org/structure/4MVF

[22] Kongsaeree P, Khongsuk P, Leartsakulpanich U, Chitnumsub P, Tarnchompoo B, Walkinshaw MD, Yuthavong Y (2005) Crystal structure of dihydrofolate reductase from *Plasmodium vivax*: pyrimethamine displacement linked with mutation-induced resistance. Proc Natl Acad Sci 102: 13046-13051.

[23] De Oliveira ME, Cenzi G, Nunes RR, Andrighetti CR, de Sousa Valadão DM, Dos Reis C, Simões CM, Nunes RJ, Júnior MC, Taranto AG, Sanchez BA (2013) Antimalarial activity of 4-metoxychalcones: Docking studies as falcipain/plasmepsin inhibitors, ADMET and lipophilic efficiency analysis to identify a putative oral lead candidate. Molecules 18: 15276-87.

[24] Lipinski CA (2004) Lead-and drug-like compounds: the rule-of-five revolution. Drug discovery today: Tech 1: 337-341.

[25] Ojo OA, Aruleba RT, Adekiya TA, Sibuyi NR, Ojo AB, Ajiboye BO, Oyinloye BE, Adeola H, Fadaka AO (2020) Deciphering the interaction of Puerarin with cancer macromolecules: an *In-silico* investigation. J Biomol Struct Dynam 2020. https://doi.org/10.1080/07391102.2020.1819425

[26] Swierczewska M, Lee KC, Lee S (2015) What is the future of PEGylated therapies? Expet Opin Emerg Drugs 20: 531–6.

[27] Wang X, Shen Y, Wang S, Li S, Zhang W, Liu X, Lai L, Pei J, Li H (2017) PharmMapper 2017 update: a web server for potential drug target identification with a comprehensive target pharmacophore database. Nucleic Acids Res 45: 356-60.

[28] Banerjee P, Kemmler E, Dunkel M, Preissner R (2024) ProTox 3.0: a web server for the prediction of toxicity of chemicals. Nucleic Acids Res.

[29] Ojo OA, Ojo AB, Maimako RF, Rotimi D, Iyobhebhe M, Alejolowo O, Nwonuma CO, Elebiyo TC (2021) Exploring the potentials of some compounds from garcina kola seeds towards identification of novel PDE-5 inhibitors in erectile dysfunction therapy. Andrologia. https://doi.org/10.1111/and.14092

[30] Ojo OA, Afon AA, Ojo AB, Ajiboye BO, Okesola MA, Aruleba RT, Adekiya TA, Oyinloye BE (2019) *Spondias mombim L*. (Anacardiaceae): chemical fingerprints, inhibitory activities and molecular docking on key enzymes relevant to erectile dysfunction and Alzheimer's diseases. J Food Biochem 43: 12772. https://doi.org/10.1111/jfbc.12772

[31] Cheng A, Dixon SL (2003) *In silico* models for the prediction of dose-dependent human hepatotoxicity. J Comput Aided Mol Des 17: 811–23.

[32] Akar S, Çırak T, Hüsunet MT, Turkdonmez I, Kenger İH, Aslan F, Kardöl A, Yıldız H, Zencir S, Emek AG, Kayraldız A (2003) Determination of mutagenic potentials of diarylmethylamine based imine compounds by ames test and computational molecular docking. Exp AppL Med Sci 4: 610-20.

[33] Nöteberg D, Schaal W, Hamelink E, Vrang L, Larhed M. High-speed optimization of inhibitors of the malarial proteases plasmepsin I and II (2003). J Comb Chem 5: 456-64.